

Different effects of valproic acid on photoreceptor loss in Rd1 and Rd10 retinal degeneration mice

Kenneth P. Mitton, Alvaro E. Guzman, Mrinalini Deshpande, David Byrd, Camryn DeLooff, Kristina Mkoyan, Paul Zlojutro, Adrienne Wallace, Brandon Metcalf, Kirsten Laux, Jason Sotzen, Trung Tran

Control of Gene Expression Laboratory and Pediatric Retinal Research Laboratory, Eye Research Institute, Oakland University, Rochester, MI

Purpose: The histone-deacetylase inhibitor activity of valproic acid (VPA) was discovered after VPA's adoption as an anticonvulsant. This generated speculation for VPA's potential to increase the expression of neuroprotective genes. Clinical trials for retinitis pigmentosa (RP) are currently active, testing VPA's potential to reduce photoreceptor loss; however, we lack information regarding the effects of VPA on available mammalian models of retinal degeneration, nor do we know if retinal gene expression is perturbed by VPA in a predictable way. Thus, we examined the effects of systemic VPA on neurotrophic factor and *Nrl*-related gene expression in the mouse retina and compared VPA's effects on the rate of photoreceptor loss in two strains of mice, *Pde6b*^{rd1/rd1} and *Pde6b*^{rd10/rd10}.

Methods: The expression of *Bdnf*, *Gdnf*, *Cntf*, and *Fgf2* was measured by quantitative PCR after single and multiple doses of VPA (intraperitoneal) in wild-type and *Pde6b*^{rd1/rd1} mice. *Pde6b*^{rd1/rd1} mice were treated with daily doses of VPA during the period of rapid photoreceptor loss. *Pde6b*^{rd10/rd10} mice were also treated with systemic VPA to compare in a partial loss-of-function model. Retinal morphology was assessed by virtual microscopy or spectral-domain optical coherence tomography (SD-OCT). Full-field and focal electroretinography (ERG) analysis were employed with *Pde6b*^{rd10/rd10} mice to measure retinal function.

Results: In wild-type postnatal mice, a single VPA dose increased the expression of *Bdnf* and *Gdnf* in the neural retina after 18 h, while the expression of *Cntf* was reduced by 70%. Daily dosing of wild-type mice from postnatal day P17 to P28 resulted in smaller increases in *Bdnf* and *Gdnf* expression, normal *Cntf* expression, and reduced *Fgf2* expression (25%). *Nrl* gene expression was decreased by 50%, while *Crx* gene expression was not affected. Rod-specific expression of *Mef2c* and *Nr2e3* was decreased substantially by VPA treatment, while *Rhodopsin* and *Pde6b* gene expression was normal at P28. Daily injections with VPA (P9–P21) dramatically slowed the loss of rod photoreceptors in *Pde6b*^{rd1/rd1} mice. At age P21, VPA-treated mice had several extra rows of rod photoreceptor nuclei compared to PBS-injected littermates. Dosing started later (P14) or dosing every second day also rescued photoreceptors. In contrast, systemic VPA treatment of *Pde6b*^{rd10/rd10} mice (P17–P28) reduced visual function that correlated with a slight increase in photoreceptor loss. Treating *Pde6b*^{rd10/rd10} mice earlier (P9–P21) also failed to rescue photoreceptors. Treating wild-type mice earlier (P9–P21) reduced the number of photoreceptors in VPA-treated mice by 20% compared to PBS-treated animals.

Conclusions: A single systemic dose of VPA can change retinal neurotrophic factor and rod-specific gene expression in the immature retina. Daily VPA treatment from P17 to P28 can also alter gene expression in the mature neural retina. While daily treatment with VPA could significantly reduce photoreceptor loss in the *rd1* model, VPA treatment slightly accelerated photoreceptor loss in the *rd10* model. The apparent rescue of photoreceptors in the *rd1* model was not the result of producing more photoreceptors before degeneration. In fact, daily systemic VPA was toxic to wild-type photoreceptors when started at P9. However, the effective treatment period for *Pde6b*^{rd1/rd1} mice (P9–P21) has significant overlap with the photoreceptor maturation period, which complicates the use of the *rd1* model for testing of VPA's efficacy. In contrast, VPA treatment started after P17 did not cause photoreceptor loss in wild-type mice. Thus, the acceleration of photoreceptor loss in the *rd10* model may be more relevant where both photoreceptor loss and VPA treatment (P17–P28) started when the central retina was mature.

Availability of the human genome sequence has accelerated the identification of genetic mutations underlying inherited and spontaneously arising retinal and vitreoretinal diseases. These diseases affect over 2-million persons worldwide [1] and affect most retinal cell types, including

the retinal pigment epithelium (RPE), photoreceptor neurons, non-photoreceptor neurons, glial cells, and cells of the retinal vasculature. As of June 2014, the number of documented genes and loci totaled 260, while 220 of these (85%) were currently identified with a specific gene (RetNet). The first human trials of gene therapy for Leber congenital amaurosis, augmenting *RPE65* gene (OMIM 180069) expression, are exciting and have restored visual function, but the treatment has not halted the degeneration of photoreceptors in patients

Correspondence to: Kenneth P. Mitton, Eye Research Institute, Room 412 Dodge Hall, Oakland University, Rochester, MI, 48309-4401. Phone: (248) 370-2079; FAX: (248) 370-4211; email: mitton@oakland.edu

treated so far [2]. Thus, enhancing photoreceptor survival across various types of retinal dystrophies of different origin may benefit from augmentation with more than one form of therapy. Targeted chemical manipulation is one way to potentially enhance the survival of retinal neurons under stresses from light, toxicity, or retinal degeneration [3].

Neurotrophic factors were one of the first families of compounds explored for their potential to improve neuron survival in genetic and oxidation-stress models of retinal degeneration. Brain-derived neurotrophic factor (BDNF) [4], glial-derived neurotrophic factor (GDNF) [5], ciliary neurotrophic factor (CNTF) [4], and fibroblast growth factor-2 (FGF2/bFGF) [4] have been injected into the vitreous, alone and in combination, to slow the rate of photoreceptor loss in the *Pde6b^{rd1/rd1}* model of rapid photoreceptor degeneration. Neurotrophic factors also have roles in retinal development where they influence the proportions of retinal cell types. CNTF can decrease the numbers of postmitotic retinal progenitor cells, adopting the rod-cell fate in the mammalian retina [6,7], yet it decreases photoreceptors in developing chick retinas [8]. Expression of neurotrophic factors from glial cells is elevated in damaged neural retinas, and these proteins can sometimes promote their own expression. BDNF and CNTF activate the extracellular-regulated kinase (ERK), protein kinase-B (Akt), and cAMP response-element binding protein (CREB) pathways to increase their own endogenous expression in *rd1* retinal explants, while they decrease FGF2 expression [3]. In wild-type retinal explants, the same treatment only changes CNTF expression [3]. Thus, the impact of neurotrophic factors on retinal gene expression may be different in a healthy versus degenerating retina.

Proteolysis limits the half-life of neurotrophic factors injected directly into the eye, and this poses a significant obstacle to adopting this therapy for humans. Encapsulation of neurotrophic factors in slow-release formulations [9] or the use of cells engineered to express neurotrophic factors are some avenues being explored to improve sustained delivery [10]. Another potential strategy would be to chemically elevate neurotrophic factor gene expression within the retina. We would categorize epigenetic therapy under the latter approach. 5-Aza-2-deoxycytidine (DAC), a DNA-methyltransferase inhibitor, and valproic acid (VPA), a histone deacetylase inhibitor (HDACi), are approved secondary treatment regimens for some leukemia, with the goal of reactivating tumor suppressor genes (*Tumor Protein p53* [OMIM 191170], *Cyclin Dependent Kinase Inhibitor 2A* [OMIM 600160]) that have become silenced by DNA-methylation [11,12]. While DAC is relatively toxic and restricted to treatment of leukemia, VPA has been used clinically for several decades as a U.S. Food

and Drug Administration-approved anticonvulsant (epilepsy), mood stabilizer (bipolar disorder), and for the prevention of migraine. VPA is a branched-chain organic acid (carboxylic) that crosses the blood-brain barrier, and its HDACi activity was discovered years after its adoption as an anticonvulsant [13]. In cell culture, VPA can increase histone acetylation, promoting an open chromatin architecture that improves accessibility of the gene for transcription. Genes that are already active with completely open chromatin architecture may not be affected by VPA's action on histone acetylation levels [14]. However, VPA can also exert unpredictable effects on gene expression by increasing posttranslational acetylation of transcription factors and other transcriptional regulatory proteins.

VPA was reported to reduce symptoms in several rodent models of stroke and amyotrophic lateral sclerosis [15,16], and it was hypothesized that VPA's beneficial effects are the result of increased expression of neurotrophic factors in the brain. However, while VPA can increase the expression of BDNF (OMIM 113505) and GDNF in neural/glia cultures in vitro, we do not know if this is true in vivo [16,17]. Recently, Zhang et al. reported that VPA prevents a drop in rat retinal *Bdnf* expression that occurs 1 week after optic nerve crush, suggesting that systemic VPA has the potential to alter neurotrophic factor gene expression in the retina [18]. While the effects of systemic HDACi treatment on gene expression in the brain and neural retina remain unclear, VPA's current medical use provides an avenue to pursue off-label clinical trials, despite our sparse understanding of its short- or long-term effects on tissue epigenomes.

Currently, we lack extensive knowledge of the roles of DNA methylation and histone acetylation in the neural retina. Our knowledge is derived from a handful of photoreceptor genes and does not cover full promoter regions [19-21]. These are significant unknowns because HDAC inhibitors alter gene expression nonspecifically and they have good or bad consequences in different cell and animal models of neurodegenerative disease [16]. In cultured retinal explants, trichostatin-A (another HDACi) caused photoreceptor loss and reduced the expression of the essential photoreceptor-specific transcription factors neural retinal leucine-zipper (NRL) and cone rod homeobox (CRX) [22]. Thus, epigenetic manipulation can be a double-edged sword. Without more studies, it is difficult to predict the safety or efficacy of HDAC inhibitors, like VPA, on retinal gene expression in a degenerating human retina. A retrospective report of several retinitis pigmentosa (RP) patients taking VPA for other indications suggested an improvement in visual acuity [23]; however, this was not a clinical trial controlling for placebo and it only involved a

handful of subjects. In humans, VPA causes a deficit in color perception and diminishes visual evoked potentials (VEP) [24-26]. In rats, VPA attenuates the ERG and VEP after several weeks of clinically relevant dosing [27].

Clinical trials of VPA are now recruiting patients with RP. While VPA does not appear to permanently harm the vision of patients with healthy retinas, we lack data to know if this is true for patients who suffer RP or any other inherited retinal dystrophy. We do know that neurotrophic factor genes have different expression patterns in the normal and degenerating neural retina, and thus the gene expression patterns in RP retinas represent a different context from a normal retina. Could VPA reduce photoreceptor loss in RP patients with one specific disease etiology but fail to affect, or even accelerate, photoreceptor loss in patients with a different disease etiology?

We started with two rodent models of retinal degeneration that are frequently used to test interventions: the *rdl* (*Pde6b*^{rd1/rd1}) and *rd10* (*Pde6b*^{rd10/rd10}) mouse strains [28]. The more recently discovered *rd10* model may be more relevant than the *rdl* model because it degenerates much later than *rdl* [28], and thus intervention treatments can be started when the retina is almost fully mature. We examined the effects of systemic VPA on the retinal expression of several neurotrophic factor and rod-specific genes, and we explored the effect of daily VPA treatment on photoreceptor loss. VPA was tested systemically because current VPA testing with human RP patients is also systemic dosing. Multiple day treatments with mice were started when approximately 95% of photoreceptors were still remaining (age P9 for *rdl* and age P17 for *rd10*). We found that a single systemic dose of VPA can have dramatic effects on gene expression in the maturing retina, and this includes both increases and decreases. Of interest to any physician considering VPA treatment of RP patients, we also found that VPA treatment had an opposite effect on the rate of photoreceptor loss in these two rodent models of retinal degeneration.

METHODS

Animal care and use: All animal care and tissue collections were performed with the approval of Oakland University's Animal Care and Use Committee and conformed to the US Department of Agriculture standards and the Association for Research in Vision and Ophthalmology statement for the use of animals in ophthalmic and vision research. CL57BL/6 and *Pde6b*^{rd1/rd1} mice were obtained from Charles River Laboratories (Wilmington, MA) and *Pde6b*^{rd10/rd10} mice from the Jackson Laboratory (Bar Harbor, ME). Both strains have mutations of the *Pde6b* (OMIM 180072) gene. Mice were

housed at Oakland University in a facility approved by the Association for Assessment and Accreditation of Laboratory Animal Care International.

VPA treatment and dosing: Initial dosing regimens were used to determine the most effective time and dosing concentration. Wild-type mouse (C57BL/6) litters were used in the initial trials. Comparisons were made between littermates receiving either VPA (Sigma-Aldrich, St. Louis, MO) or vehicle (PBS, 138 mM NaCl, 2.7 mM KCl, 10 mM NaPO₄, 2.2 mM KPO₄). All treatments with VPA were systemic intraperitoneal (IP) injections. The effects of a single systemic VPA dose were examined on postnatal and adult mice to determine if VPA had any potential to alter retinal gene expression. Mouse strains were also subjected to treatment protocols, dosing once per day using one of two treatment windows, referred to as early treatment (ages P9 to P21) and late treatment (ages P17 to P28). These windows were selected to correspond to the onset and loss of most photoreceptors in the two degeneration models, with early and late corresponding to *rdl* and *rd10*, respectively. An intermediate dose of VPA, which could alter neurotrophic factor gene expression, was used for daily VPA treatment of *Pde6b*^{rd1/rd1}, *Pde6b*^{rd10/rd10}, and wild-type (C57BL/6) mice.

RNA extraction from mouse neural retinas: Neural retinas were collected by dissection of freshly enucleated eyes in PBS (calcium and magnesium free) at room temperature and were isolated free of ciliary body, RPE, and optic nerve. Retinas were fast frozen inside Eppendorf tubes held at dry ice temperature. Frozen retinas were stored at -70 °C until extraction for RNA. Total RNA was extracted from frozen retinas with the Absolute RNA Mini-Prep Kit reagents (Agilent Technologies, Santa Clara, CA). Single retinas were homogenized in 200 µl of lysis buffer, or pairs of retinas were homogenized in 300 µl of lysis buffer.

Real-time quantitative PCR: A two-step process was used, making cDNA first, followed by real-time PCR using Taqman chemistry with separate probes for the gene of interest and the endogenous *Actb* gene (β-actin, OMIM 102630) for normalization. The AffinityScript qPCR cDNA Synthesis Kit (Agilent Technologies) was used to prepare first-strand cDNA from 500 to 1,000 ng of total RNA, with oligo-dT priming under the following reaction conditions: 25 °C for 5 min, 42 °C for 20 min, 95 °C for 5 min, 10 min at 10 °C. Expression of specific genes was analyzed by multiplex real-time PCR using gene-specific FAM-labeled Taqman probe/primers in a duplex reaction with *Actb* VIC-labeled probe/primers following the manufacturer's protocol (Applied Biosystems, Foster City, CA). Reactions were run with an Agilent Mx3000P real-time PCR system. For PCR, cDNAs

TABLE 1. GENE EXPRESSION PRIMER AND PROBE SETS USED FOR RT-qPCR.

Gene name	Assay ID	Exons spanned	Amplimer size (bp)
<i>Cntf</i>	Mm00446373_m1	1, 2	82
<i>Gdnf</i>	Mm00599849_m1	1, 2	101
<i>Bdnf</i>	Mm04230607_s1	2	92
<i>Fgf2</i>	Mm00433287_m1	1, 2	61
<i>Rho</i>	Mm00520345_m1	1, 2	86
<i>Actb</i>	Mm00607939_s1	6	115
<i>Nrl</i>	Mm00476550_m1	3-4	61
<i>Mef2c</i>	Mm01340839_m1	5-6	137
<i>Crx</i>	Mm00483995_m1	2-3	63
<i>Nr2e3</i>	Mm00443302_g1	4-5	124
<i>Pde6b</i>	Mm00476679_m1	12-13	74

were first diluted 5-times with deionized water for neurotrophic factor gene expression or diluted 50-times with deionized water for *Rho* (OMIM 180380), *Nrl* (OMIM 162080), and *Mef2c* (OMIM 600662), *Crx* (OMIM 602225), *Nr2e3* (OMIM 604485), and *Pde6b* gene expression. Gene expression was normalized to endogenous *Actb* expression measured in the same PCR tube. Pre-inventoried probe sets or custom assays were produced for the genes of interest. The splice-specific Taqman assays used are listed in Table 1.

Virtual microscopy for morphology analysis: Eenucleated whole eyes were fixed for 15 min in Davison's fixative, the cornea was removed, and fixation continued up to 2 h. Some eyes were fixed whole for 3 h or retinal eye cups were fixed for 2 h in Davidson's fixative. Fixed tissues were processed for paraffin sections and stained with hematoxylin and eosin. Sections were obtained near the optic nerve region to obtain full cross-sections of retina (7- μ m thick) from periphery to periphery. Whole slides were digitized using a 20X objective lens and an Olympus SL120 Virtual Microscopy Slide Scanner (Center Valley, PA) and saved in the vsi-file format. Digital files were managed and analyzed using Leica (Slidepath) Digital Image Hub and Digital Slide Box (DSB) web servers, with the Safari web browser (Apple, Cupertino, CA). Measurements of outer nuclear layer (ONL) thickness were made from vsi-format files using digital calipers in DSB, starting 100 μ m from the first photoreceptor nucleus adjacent to the optic nerve (disc) and then every 200 μ m toward the retinal periphery in both directions. Penultimate measurements were made within 100 μ m from each peripheral end. Measurements of ONL thickness, calculations of averages, *t*-test calculations, and generation of spiderogram graphs were accomplished using Microsoft Excel.

Animal preparation for ERG analysis: ERG analysis of *Pde6b*^{rd10/rd10} mice was completed in the Pediatric Retinal Research Lab's retinal imaging and ERG suite of the Eye Research Institute (ERI). This workspace is equipped with dim red room lighting (variable 4–15 lux). (For reference, regular fluorescent lighting is 400 lux). After 2 h of dark adaptation, pupils were dilated with a sequential application of tropicamide and phenylephrine eye drops. Short-term anesthesia, 30 min, was induced by a single injection (IP) of 50 mg/kg ketamine HCl and 7 mg/kg xylazine. Upon loss of the blink reflex, corneas were protected by Genteal lubricant solution.

Focal ERG: Focal ERG recordings were from dark-adapted mice (age P25), using a Micron-III camera-mounted focal ERG system (Phoenix Research Labs, Pleasanton CA). Aiming of the light stimulus was accomplished by viewing the retina with dim red-filtered LED illumination, high camera gain, and 15-frame video averaging. A circular LED white-light stimulus of 6 disc-diameters was projected onto the central retina (30-msec duration) with a bright intensity setting corresponding to an energy delivery of 121,597 cd-sec/m² of projected retinal area (measured by Greg Sprehn, Phoenix Research Labs, and Ken Mitton, ERI). Mice were maintained on a regulated temperature pad at 37 °C. The lens mount of the focal ERG provided the gold corneal electrode. Platinum cutaneous needle electrodes were used for the reference and ground and were inserted into the head cap and hind flank skin. Triggering of the light stimulus and acquisition of the corneal voltage trace were accomplished with LabScribe2 software equipped with the Phoenix Research Labs' ERG module. Twenty stimulus traces were averaged to obtain the ERG trace. Amplitudes of the A-wave and B-wave were determined from averages of the left and right eyes for each mouse.

Ganzfeld (full-field) ERG: Mice, at age P27, were positioned on a custom rodent platform with an integrated heater (37 °C) under a Diagnosys Color Dome illumination system, controlled by an Espion-III ERG system and software (Diagnosys LLC, Lowell, MA). ERG recordings were collected from the left and right eyes simultaneously using an intensity series of white-light flashes. Light flashes were 10 msec in duration, and final ERG traces were produced from four time-averaged traces at each intensity. Measurement corneal electrodes were gold wire fashioned into circular loops to fit around the cornea. Platinum needle electrodes were used for the reference and ground and were inserted into the head cap and hind flank skin.

Spectral domain optical coherence tomography analysis: Pupils were dilated with a sequential application of tropicamide and phenylephrine eye drops. Short-term anesthesia, 30 min, was induced by a single injection (IP) of 50 mg/kg ketamine HCl and 7 mg/kg xylazine. Upon loss of the blink reflex, corneas were protected by an artificial tears solution (CVS Dry Eye Relief Eye Drops, CVS Health, Woonsocket, RI). Mice were positioned in a custom support (Bioptigen, Durham NC), and OCT scans were obtained with a Biop-tigen Envisu-R2200 model SD-OCT system, equipped with a custom lens for the mouse eye. A rectangular scan pattern of 1.4 mm×1.4 mm was used, with ten horizontal B-scan locations averaging ten B-scans per location at a resolution of 1,000 A-scans/B-scan. Retinal layers were marked and measured from averaged OCT images, using InVivoVue Diver 2.0 software (Biop-tigen). Using the Diver software, a 5×5 position grid was centered on the optic disc viewed en face. The depths of all retinal layers were manually marked at each grid position (24 positions), except the central position over the disc. Layers marked were ganglion cell layer, inner plexiform layer, inner nuclear layer (INL), outer plexiform layer (ONL), photoreceptor inner segments, photoreceptor outer segments, and the RPE. Measurements were exported into Microsoft Excel, and the average ONL thickness was calculated for each eye and then averaged for each animal.

RESULTS

Effect of systemic VPA (single dose) on neurotrophic factor gene expression in the mouse neural retina: The expression of neurotrophic factor genes in the neural retinas of wild-type mice (C57BL/6) were examined at two postnatal ages, P12 and P15, just 18 h after a single systemic injection of VPA. Littermates at each age were injected (IP) with either a high dose of VPA (415 mg/kg), low dose of VPA (250 mg/kg), or vehicle (PBS) as controls. Results were the same at both ages, and a graph showing the average of these experiments

is presented in Figure 1A. There was a dose response to VPA, with statistically significant increases in the relative expression of *Gdnf* and *Bdnf* as measured by real-time PCR. At the higher VPA dose, *Gdnf* (OMIM 600837) expression increased 12-fold ($p < 0.001$, *t* test) and *Bdnf* expression increased twofold ($p < 0.01$), compared to PBS-injected littermates. *Cntf* (OMIM 118945) gene expression decreased 80% ($p < 0.001$) compared to PBS-injected littermates. In contrast to younger neural retinas, the retinal expression of these genes in adult retinas was not perturbed substantially by a single dose. While there was a trend to shift the expression of neurotrophic factors, the changes were not judged to be statistically significant compared to PBS-injected animals (data not shown).

Effect of systemic VPA (single dose) on rod-specific transcription factor gene expression in the neural retina: We examined the effect of systemic VPA on the expression of the *Nrl* gene in vivo. As for the neurotrophic factor genes above, the effect of a single systemic dose of VPA on *Nrl* expression was the same in postnatal mice at P12 or P15. Within 18 h, the higher VPA dose (450 mg/ml) diminished *Nrl* gene expression by 50% ($p < 0.003$) compared to PBS-injected littermates (Figure 1B). Compared to neurotrophic factor gene expression, *Nrl* gene expression was more resistant to the effects of VPA and was not reduced at the lower VPA dose tested (250 mg/kg).

We also examined the NRL-dependent expression of the *Mef2c* gene in rod photoreceptors, using an assay we designed previously for a rod-specific transcript from the *Mef2c* gene [29]. Mice injected with a single systemic VPA dose at age P15 had reduced *Mef2c* gene expression (Figure 1C). We did not examine the expression of *Mef2c* in mice injected younger than P15 since NRL-dependent expression of *Mef2c* is essentially nonexistent before this postnatal age. As for the *Nrl* gene, *Mef2c* expression was decreased 50% ($p < 0.05$) at the higher VPA dose but was not perturbed by the lower dose. Average *Rho* gene expression was slightly lower (not significant) in VPA-dosed mice in age P12 retina 18 h post-injection compared to PBS-dosed littermates (Figure 1D).

*Effect of VPA (single dose) on neurotrophic factor gene expression in the immature *Pde6b*^{rd1/rd1} retina:* Even though *rdl* retinas can have higher neurotrophic factor gene expression compared to wild-type retinas, we found that a single systemic dose of VPA (350 mg/kg) could still shift *Gdnf* expression and decrease *Cntf* gene expression in the *rdl* retina relative to PBS-treated *rdl* littermates (age P15), 18 h after injection (IP) Figure 2. We also examined retinal *Fgf2* (OMIM 134920) gene expression because *Fgf2* expression is often reported to increase during retinal damage and degeneration compared to wild-type retinas [30,31]. VPA-treated

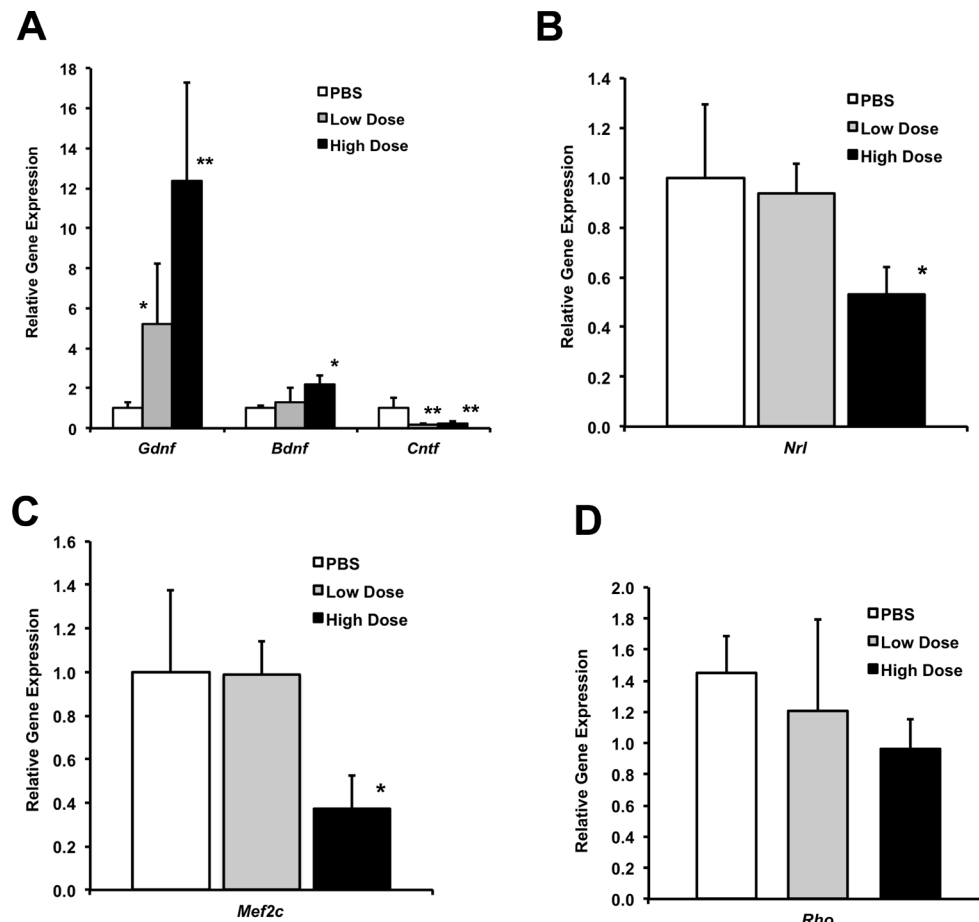


Figure 1. Effect of a single systemic dose of valproic acid (VPA) on neurotrophic factor gene expression and rod-specific gene expression in the immature retina of wild-type mice. A: Expression of the *Gdnf*, *Bdnf*, and *Cntf* genes in the neural retinas of wild-type mice (C57BL/6) was examined at two postnatal ages, P12 (n = 2/group) and P15 (n = 3/group), 18 h after one systemic VPA dose. Littermates at each age received a high dose (415 mg/kg), low dose (250 mg/kg), or PBS. The graph shows the average of these experiments (mean±standard deviation [SD]). Gene expression was normalized to endogenous *Actb* expression and is plotted relative to control PBS-injected littermates (*t* test, * p<0.01, ** p<0.001, relative to PBS). B: Retinal *Nrl* gene expression at two postnatal ages, P12 (n = 2/group) and P15 (n = 3/group), 18 h after a single systemic injection (IP) of VPA. Littermates within each age received a high dose (VPA 415 mg/kg), low dose (VPA 250 mg/kg), or

PBS only (control). The graph shows the average of the two experiments (mean±SD; *t* test, *p<0.05 relative to PBS). C: Rod-specific *Mef2c* gene expression at age P15, 18 h after treatment with a high dose (VPA 415 mg/kg), low dose (VPA 250 mg/kg), or control (PBS) (*t* test, *p<0.05 relative to PBS, n = 3/group). D: *Rhodopsin* gene (*Rho*) expression in the P12 neural retina, 18 h after injection (IP) with a high or low dose of VPA compared to PBS only (mean±SD; n = 2/group).

Pde6b^{rd1/rd1} mice had 75% lower retinal *Fgf2* gene expression compared to their PBS-treated littermates (P15).

Effect of systemic VPA treatment (later treatment, P17–P28) on retinal morphology and gene expression in wild-type mice: We used an intermediate dose (350 mg/kg/day) for daily treatment of wild-type mice with VPA as it involved multiple doses delivered from age P17 to age P28. We employed SD-OCT to confirm that VPA treatment started at P17 has no effects on retinal morphology before collecting the tissue for gene expression analysis. Based on an average of 24 different OCT measurement locations from both eyes of each mouse, the average ONL thickness was exactly the same comparing VPA-treated (63±2 μm, n = 3) and PBS-treated (63±2 μm, n = 3) littermates. Examples of high-resolution B-scans of a VPA-treated and PBS-treated littermate are shown in Appendix 1. We compared the expression of several neurotrophic factors and rod photoreceptor specific genes from these same mice

(Figure 3). Retinal *Bdnf* and *Gdnf* gene expression was elevated 1.6- and twofold, respectively, in the VPA-treated littermates. Retinal *Cntf* gene expression of VPA-treated mice was the same as their PBS-treated littermates, while *Fgf2* gene expression was diminished by 25%. Most notable was a 50% reduction in endogenous *Nrl* gene expression by the end of the dosing period. In contrast, *Crx* gene expression was the same comparing VPA-treated and PBS-treated littermates. Both *Rhodopsin* and *Pde6b* gene expression in VPA-treated mice attained the same level as their PBS-treated littermates by age P28. In contrast, the NRL-dependent and rod-specific expression of the *Mef2c* gene was reduced by 90%. Expression of the rod-specific co-activator/co-repressor *Nr2e3* gene was also reduced by 55% in VPA-treated mice compared to PBS-treated littermates (Figure 3).

Effect of systemic VPA (multiple doses) on the rate of photoreceptor loss in *Pde6b*^{rd1/rd1} mice: The *Pde6b*^{rd1/rd1} strain

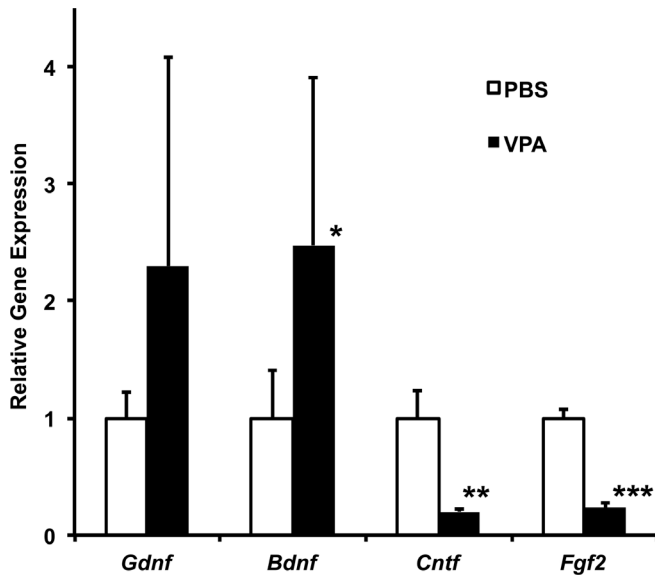


Figure 2. Effect of a single systemic dose of valproic acid (VPA) on retinal neurotrophic factor gene expression in the *Pde6b^{rd1/rd1}* mouse strain. A single dose of VPA (350 mg/kg) was administered by intraperitoneal injection, and neural retinas were collected 18 h after the injection at age P15. Gene expression relative to PBS-injected littermates was measured using real-time PCR for the gene of interest (*Gdnf*, *Bdnf*, *Cntf*, *Fgf2*) and was normalized to *Actb* expression (mean±standard deviation; n = 3/group, *t* test, *p<0.08, **p<0.005, ***p<0.001, relative to PBS).

represents an aggressive model of photoreceptor degeneration and is frequently used to test interventions for a potential to slow less aggressive retinal degenerations. Mice homozygous

for the *rd1* mutation have a truncating mutation in the *Pde6b* gene that inactivates visual transduction and causes a rapid loss of rod photoreceptors, starting at age P7 [32,33]. By age P33, more than 99% of rods have degenerated and 50%–70% of cone photoreceptors remain. We have previously used this strain to demonstrate novel rod-specific expression of genes during photoreceptor maturation in the mouse [29,34].

We treated *Pde6b^{rd1/rd1}* mice with daily doses of VPA and compared results to that of PBS-injected (control) littermates. We used an intermediate dose (350 mg/kg) for treatment for multiple dosing. Daily VPA injections (IP) were started at age P9 and continued to age P21 when retinal morphology was evaluated (12 continuous days of dosing). VPA treatment resulted in a significant reduction in the rate of photoreceptor loss (Figure 4A). Retinas from PBS-injected littermates had a single row of photoreceptor nuclei, as expected, by age P21 in the *Pde6b^{rd1/rd1}* strain. In contrast, the retinas from VPA-treated littermates had three to four rows of photoreceptor nuclei remaining in the ONL. Measurements from full retinal sections showed that VPA-treated littermates had a significantly thicker ONL from periphery to periphery, shown by the spiderogram graphs in Figure 4B. Virtual microscopy images of whole retinal cross-sections from VPA-treated (daily) and PBS-treated *Pde6b^{rd1/rd1}* mice are available in Appendix 2 and Appendix 3.

Rhodopsin gene expression levels were measured by real-time PCR to confirm that extra rows of photoreceptor nuclei in VPA-treated animals were rods. *Rhodopsin* expression,

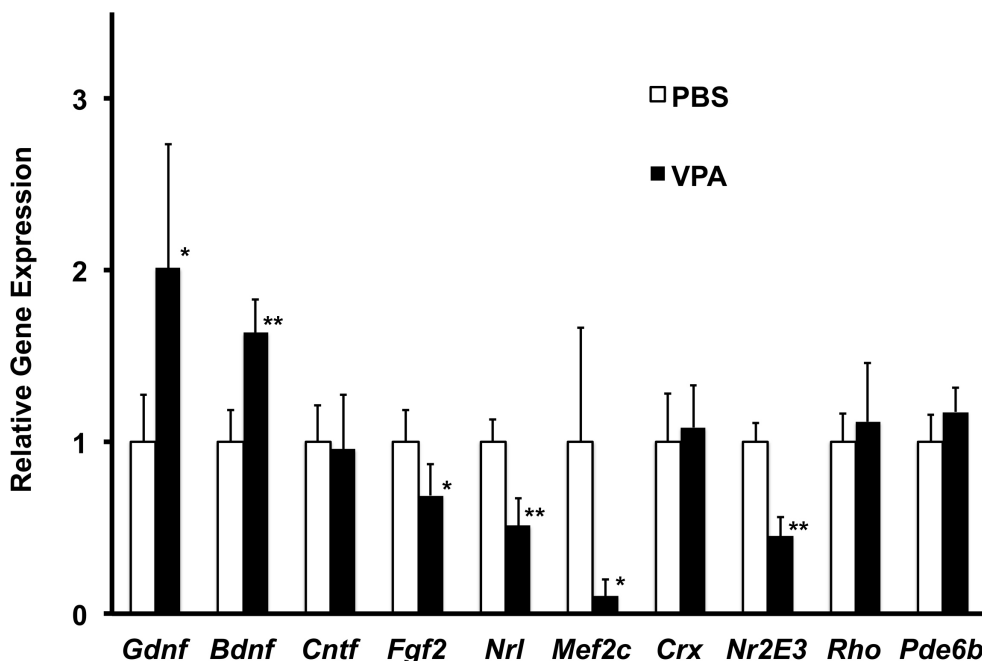


Figure 3. Effect of daily systemic valproic acid (VPA; P17–P28, late treatment) on neurotrophic factor and rod-specific gene expression in the wild-type mouse retina. A daily dose of VPA (350 mg/kg) was administered by intraperitoneal injection starting at age P17. Littermates received injections of PBS only. Gene expression, relative to PBS-injected littermates at age P28 was measured using real-time PCR for the gene of interest (*Gdnf*, *Bdnf*, *Cntf*, *Fgf2*, *Mef2c*, *Nrl*, *Crx*, *Nr2E3*, *Rho*, *Pde6b*) and was normalized to *Actb* expression (mean±standard deviation; n = 3/group, *t* test, *p<0.05, **p<0.01, relative to PBS).

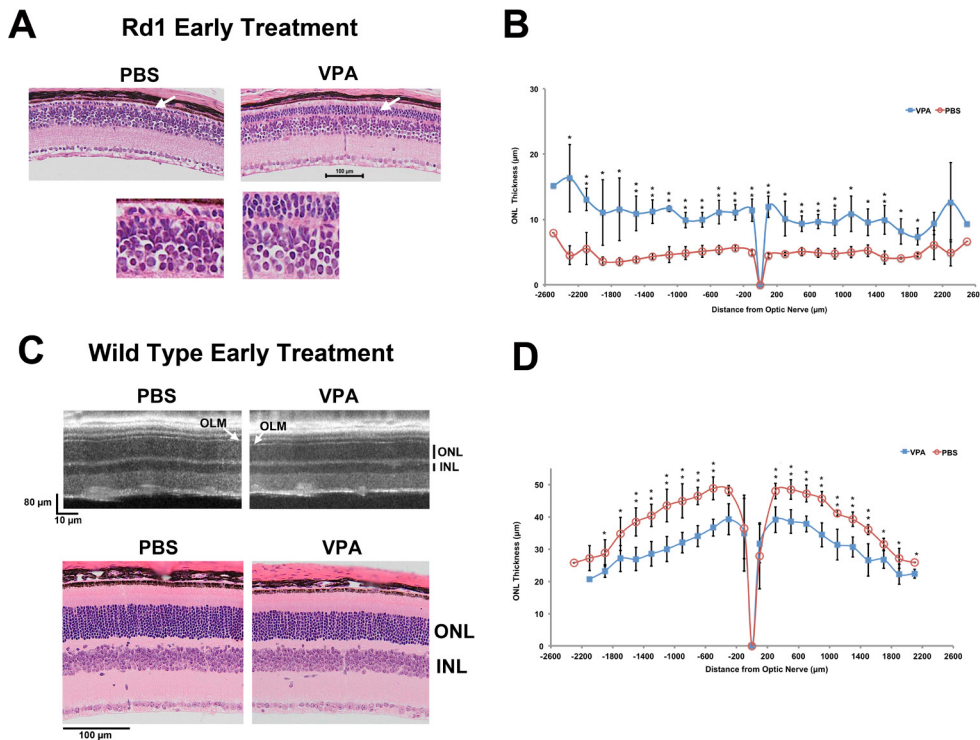


Figure 4. Daily systemic valproic acid (VPA; P9–P21, early treatment) reduced the rate of photoreceptor loss in *Pde6b*^{rd1/rd1} mice. **A:** Systemic VPA treatment of *Pde6b*^{rd1/rd1} mice was 350 mg/kg/day (IP injection) from age P9 to P21 (early treatment). Three to four extra layers of photoreceptor cells (nuclei) remained in VPA-treated mice compared to PBS-treated controls. Examples of retinal sections (P21) are shown from a VPA-treated and PBS-treated littermate (control). White arrows indicate the outer nuclear layer (ONL). Regions of the ONL just left of the white arrows are also shown below at higher magnification (sections are paraffin, hematoxylin and eosin stained). **B:** Spiderogram graphs showing the thicker ONL in *Pde6b*^{rd1/rd1} mice after daily

systemic VPA early treatment (P9–P21) compared to PBS-treated littermates. ONL thickness is plotted at 200- μ m intervals from the optic nerve to the retinal periphery, using a virtual microscopy of full retinal histology sections (paraffin, hematoxylin and eosin stained; $n = 3$ /group, t test, * $p < 0.05$, ** $p < 0.01$, relative to PBS). **C:** Systemic VPA treatment of wild-type mice from age P9 to P21 (early treatment) resulted in a 10%–20% loss of photoreceptor cells. Example SD-OCT images (P21) and retinal histology sections (P21) from the same VPA-treated and PBS-treated littermates are shown, confirming thinning of the ONL in vivo (INL, inner nuclear layer; OLM, outer limiting membrane). **D:** Spiderogram graphs showing the thinner ONL in wild-type mice after daily systemic VPA early treatment (P9–P21) compared to PBS-treated littermates ($n = 4$ /group, t test, * $p < 0.05$, ** $p < 0.01$, relative to PBS).

relative to *Actb* expression, was fivefold higher in VPA-treated *rd1* mice compared to their PBS-treated littermates ($p < 0.001$, t test): 0.69 ± 0.19 for VPA-treated mice ($n = 3$) and 0.13 ± 0.03 for PBS-treated controls ($n = 3$).

Even though the postmitotic photoreceptor cell population is present by age P9 in the mouse retina, treatment testing with the *rd1* model still has substantial overlap with retinal maturation. Thus, we also subjected wild-type mice to VPA early treatment (P9–P21) to confirm that VPA was not generating additional photoreceptors that might give the appearance of photoreceptor preservation in the *rd1* model. Early VPA treatment did not result in the formation of more photoreceptors. As reported for the TSA treatment of newborn mouse retinal explants [22], we found that early VPA treatment was toxic to the maturing wild-type retina and resulted in a significant loss of photoreceptors. A reduction of ONL thickness in VPA-treated mice compared to PBS-treated littermates was visible in SD-OCT images in vivo and in retinal histology (Figure 4C). Spiderogram graphs show the corresponding thinning of the ONL across the entire retina

(Figure 4D). Thinning of the ONL in wild-type mice from early VPA treatment (P9–P21) was confirmed in a repeated test with a different litter (data not shown).

We also tested daily VPA treatment of *Pde6b*^{rd1/rd1} mice starting later (P14 to P21), and dosing every second day (P14–P21). In both cases, we observed a reduction in photoreceptor loss for VPA-injected littermates compared to their PBS-injected littermates (Figure 5A,B), although these treatments were less effective than the daily VPA dosing from age P9 to P21.

*Effect of systemic VPA (multiple doses) on the rate of photoreceptor loss in *Pde6b*^{rd10/rd10} mice:* Even though VPA treatment reduced photoreceptor loss in the *rd1* model starting treatment later at age P14, rod photoreceptors are typically lost by age P21 in untreated *Pde6b*^{rd1/rd1} mice. Thus, most of the degeneration and VPA treatment occurs in an immature retina, i.e., before P21. We then turned to the *Pde6b*^{rd10/rd10} model to determine if systemic VPA could also reduce

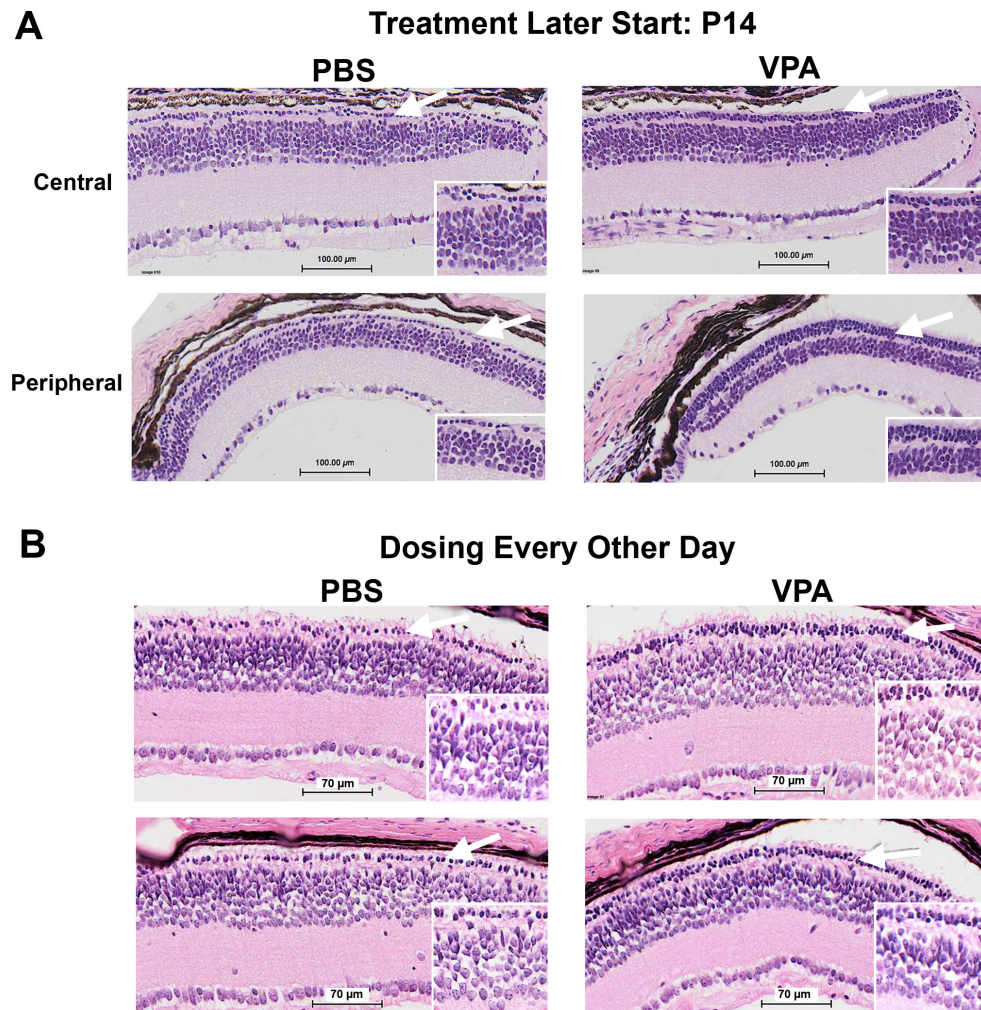


Figure 5. Valproic acid (VPA) treatment using alternative dosing schedules started later or every second day reduced the rate of photoreceptor loss in *Pde6b^{rd1/rd1}* mice. White arrows indicate the outer nuclear layer and regions shown at higher magnification (inserts). **A:** Daily VPA injections (350 mg/kg/day IP) started later from age P14 to P21. Two to three additional layers of photoreceptor cells (nuclei) remained in VPA-treated littermates compared to PBS-treated controls. **B:** VPA treatment with dosing every second day (350 mg/kg) and the treatment period starting later from age P14 to P21 also reduced the rate of photoreceptor loss (sections are paraffin, hematoxylin and eosin stained).

photoreceptor loss when most of the degeneration occurs in a mature neural retina with visual function.

Rd10 mice were treated with VPA from age P17 to P28. During this treatment, we monitored retinal function in vivo at age P25 using focal ERG to stimulate a circular area of retina equivalent to 6 disc-diameters and centered about the optic disc. A bright flash intensity was used with dark-adapted mice to obtain the combined rod and cone response. VPA treatment reduced the average A-wave amplitude by 45% ($p = 0.06$, t test) and the average B-wave amplitude by 15% ($p = 0.14$, t test) compared to PBS-treated littermates (see Table 2). This suggested a possible diminished visual function in VPA-treated littermates. Because the already subnormal ERG response would diminish with age, we used bilateral full-field ERG for evaluation at age P27 and could test both eyes simultaneously over a range of light intensity. While amplitudes of the photoreceptor-derived A-wave were weak by this age, the B-wave amplitudes were measurable

over a range of light intensities. The average difference in B-wave amplitude between VPA-treated and PBS-treated littermates at seven light intensities was $36 \pm 18 \mu\text{V}$ ($p = 0.005$, t test), with the PBS-treated group having higher amplitudes (Figure 6A). ERG traces were similar between contralateral eyes, and examples are shown in Figure 6B.

ERG analysis suggested slightly reduced retinal function in VPA-treated *Pde6b^{rd10/rd10}* mice compared to PBS-treated littermates. Eyes from *Pde6b^{rd10/rd10}* mice, treated from P17 to P28, were then harvested for assessment of retinal morphology. *Pde6b^{rd10/rd10}* mice typically have several rows of photoreceptor nuclei remaining at age P28, and this was also our observation for PBS-treated littermates (Figure 7). VPA-treated *Pde6b^{rd10/rd10}* mice displayed one to two fewer rows of photoreceptor nuclei compared to their PBS-treated littermates, mostly in the central to middle retinal region (Figure 7A,B). ONL thickness was measured using retinal sections of the same ERG-tested mice, and the spidergram

TABLE 2. CENTRAL FIELD FOCAL-ERG A- AND B-WAVE AMPLITUDES IN *PDE6BRD10/RD10* MICE UNDER SYSTEMIC VPA-TREATMENT (AGE P17-P28, LATE DOSING), MEASURED AT AGE P25.

Group	B-wave ($\mu\text{V} \pm \text{SD}$)	A-wave ($\mu\text{V} \pm \text{SD}$)
VPA (n=3)	119±18.2	-13.3±5.7
PBS (n=2)	140±17.0	-25.0±7.1
P value (<i>t</i> test)	0.14	0.06

Focal-ERG tests were completed at age P25. Mixed rod-cone responses of dark-adapted retinas, using a circular bright light flash stimulus of 6 optic disc diameters, centered on the optic disc.

graphs are shown in Figure 8A. A slight but statistically significant decrease in ONL thickness was detected at several measurement locations in VPA-treated mice compared to their PBS-treated littermates. Repetition of the treatment with an additional litter confirmed that daily VPA treatment

from age P17 to P28 did not slow photoreceptor loss in the *Pde6b^{rd10/rd10}* strain and resulted in a thinner ONL compared to PBS-treated littermates. Examples of retinal histology from the repeated experiment are shown in Appendix 4.

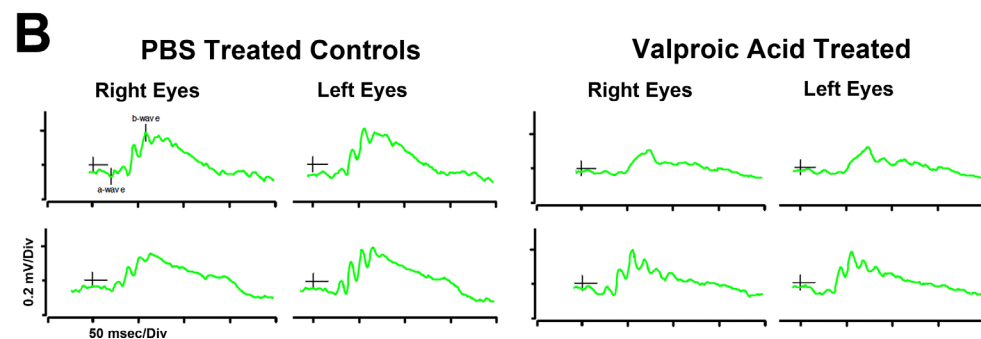
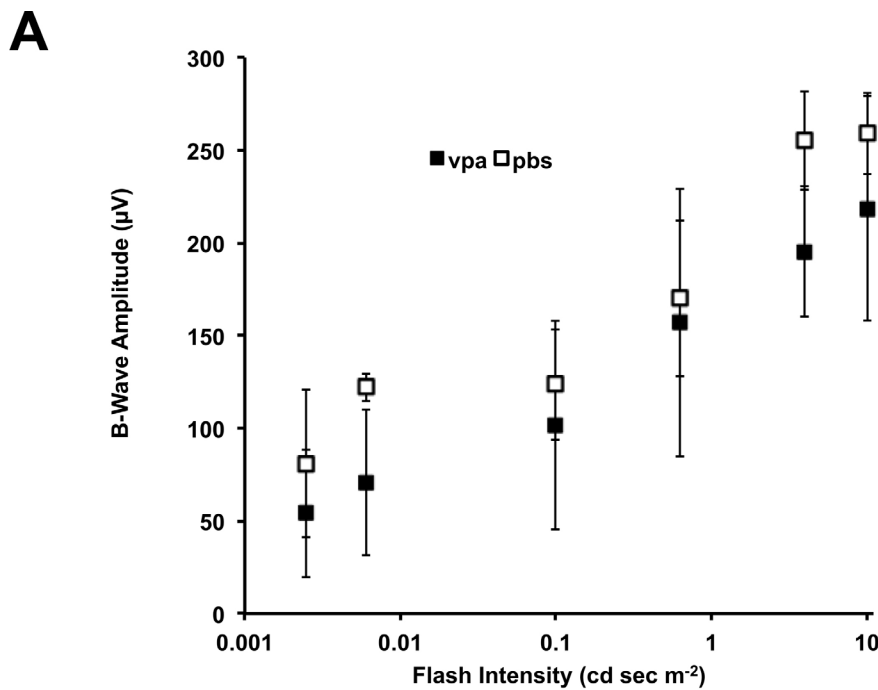


Figure 6. Full-field (ganzfeld) ERG testing of *Pde6b^{rd10/rd10}* mice treated with systemic valproic acid (VPA; P17–P28, later treatment). Bilateral full-field electroretinography (ERG) testing was completed on dark-adapted mice at age P27. **A:** Graph of the dark-adapted B-wave amplitudes from VPA-treated (n = 3) and PBS-treated (n = 2) littermates (mean±standard deviation) at age P27. Amplitudes for each individual were calculated as an average of both eyes. VPA-treated mice had reduced amplitudes relative to PBS-treated controls over the range shown. **B:** Examples of bilateral full-field ERG traces from VPA-treated and PBS-treated littermates for the dome flash intensity of 4 cd-sec/m². ERG responses were similar between contralateral eyes.

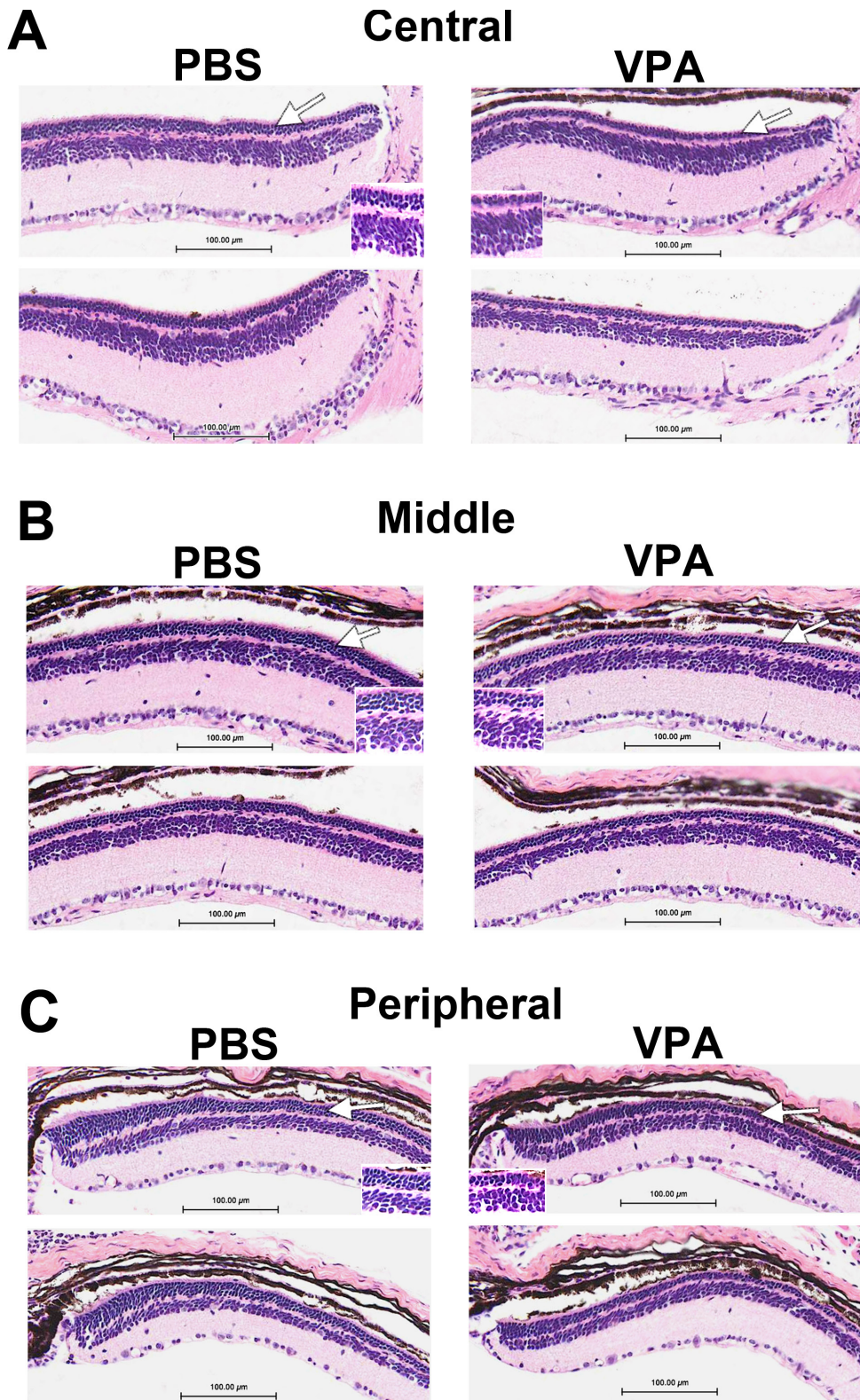


Figure 7. Daily systemic valproic acid (VPA; P17–P28, later treatment) increased the rate of photoreceptor loss in *Pde6b^{rd10/rd10}* mice. Retina sections are shown from two different treated and two different control littermates at age P28. White arrows indicate the outer nuclear layer and regions shown at higher magnification (inserts). Daily injections (IP) of 350 mg/kg VPA from age P17 to P28. **A:** Central retina; **B:** middle retina; **C:** peripheral retina (sections are paraffin, hematoxylin and eosin stained).

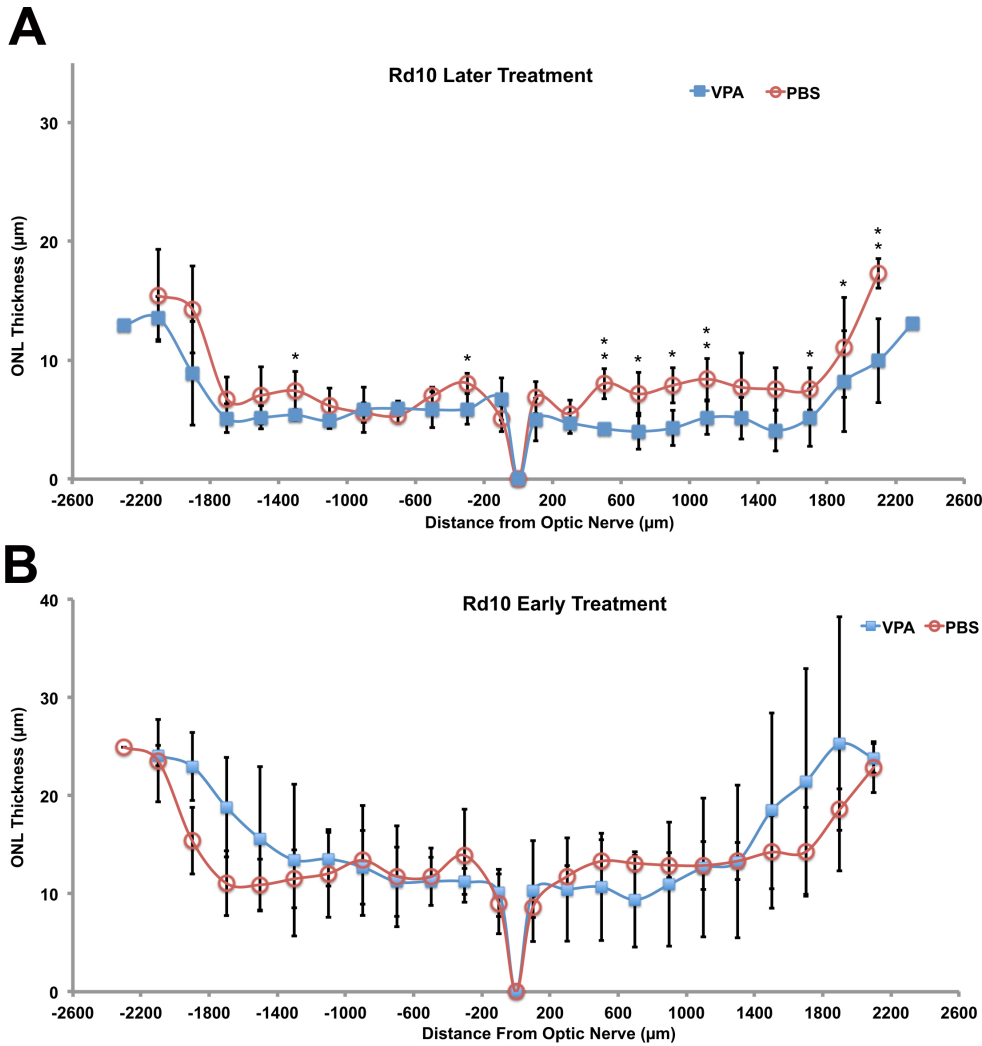


Figure 8. Outer nuclear layer thickness in *Pde6b^{rd10/rd10}* mice after later (age P17-P28) and early (age P9-P21) systemic valproic acid (VPA) treatment. Spiderogram graphs of outer nuclear layer (ONL) thickness measured from periphery to periphery in *Pde6b^{rd10/rd10}* mice treated with systemic VPA or PBS (control littermates). **A:** Slightly thinner ONL in VPA-treated *Pde6b^{rd10/rd10}* mice compared to PBS-treated littermates at age P28, after late dosing (age P17-P28; n = 4 VPA, 3 PBS; *t* test, **p*<0.05, ***p*<0.01, relative to PBS). **B:** ONL thickness in VPA-treated and PBS-treated littermates at age P21, after early treatment (age P9-P21) (n = 3 VPA, 4 PBS; *t* test, **p*<0.05, ***p*<0.01, relative to PBS).

While the initial VPA treatment window for *rd10* mice (P17–P28) was later than that used for *rd1*, to account for the later onset of photoreceptor loss in the *rd10* model we also tested *Pde6b^{rd10/rd10}* mice using the earlier treatment window (P9–P21). This did not result in any significant differences in ONL thickness between VPA-treated and PBS-treated littermates. However, the average ONL thickness of VPA-treated mice was slightly greater (not significant) than their PBS-treated littermates in the peripheral retina (Figure 8B).

DISCUSSION

Systemic VPA treatment can change gene expression in the neural retina: Until now, the hypothesis that VPA can induce changes to neurotrophic factor gene expression *in vivo* was mostly derived from experiments using primary cultures of neurons or mixed glial/neurons [17,35,36]. Our results here demonstrate that retinal and photoreceptor-specific gene

expression can be altered by systemic VPA treatment in the immature developing retina and in the mature retina. A single dose of VPA was sufficient to affect neurotrophic factor gene expression in the immature retinas of wild-type and *Pde6b^{rd1/rd1}* mice, including *Bdnf*, *Gdnf*, and *Cntf*. Two of these genes encode proteins (GDNF, CNTF) that can slow retinal degeneration in *Pde6b^{rd1/rd1}* mice when the proteins are injected into the vitreous humor or subretinal space [4,5,10]. While gene expression in the adult retina was resistant to a single dose of VPA, daily VPA treatment of wild-type mice from P17 to P28 caused significant changes to neurotrophic factor gene expression. In VPA-treated littermates, *Gdnf* gene expression was elevated twofold compared to PBS-treated littermates and *Bdnf* gene expression was elevated 1.6-fold. While *Cntf* gene expression was normal at the end of the P17–P28 dosing period, *Fgf2* expression was decreased by 25% (Figure 3).

VPA has the potential to affect gene expression by altering the extent of histone acetylation. We also know that photoreceptor genes are potential VPA target genes because we have previously shown that increased H3K9 acetylation is a fundamental feature in the developmental activation of photoreceptor-specific gene promoters in vivo, including *Rhodopsin*, *Pde6b*, and *Mef2c* [29,34]. Currently, we do not know if VPA treatment causes a long-term reduction in lysine acetyltransferase activity within the neural retina. However, our results include examples of decreased gene expression as well as increased gene expression from systemic VPA treatment. In addition to the decreased expression of *Fgf2* in wild-type retina, after VPA treatment from P17 to P28, *Nrl* gene expression was decreased by almost 50%. NRL is essential for activating the expression of all rod-specific genes versus cone-specific genes in photoreceptor progenitor cells [37-40]. In contrast, *Crx* gene expression was not affected by systemic VPA treatment. While this reduction in *Nrl* expression did not preclude a normal level of *Rho* and *Pde6b* expression by age P28, the rod-specific expression of *Mef2c* and *Nr2e3* was reduced substantially (Figure 3).

This greater sensitivity of *Mef2c* and *Nr2e3* gene expression to VPA treatment may reflect their relatively greater dependence upon NRL versus CRX for their own expression. Rod-specific expression of *Mef2c* transcripts begin late at age P15. Recently, we described a novel rod-specific promoter in the *Mef2c* gene that binds NRL in vivo relatively late in photoreceptor maturation [29]. *Nr2e3* expression is also restricted to rod photoreceptors and is dependent upon NRL. NRL-null mice (*Nrl*^{-/-}) lack expression of *Nr2e3* and rod-specific transcripts from the *Mef2c* gene [29,39].

CRX is a pioneer transcription factor that binds to photoreceptor gene promoters and recruits histone acetyltransferases. Subsequent to CRX binding at the *Rhodopsin* promoter, histones are acetylated and then NRL binds to the promoter [20]. CRX works synergistically with NRL to activate the expression of *Rho* and *Pde6b* around age P4 in the mouse [41,42]. Our analysis found that *Crx* gene expression (mRNA) was high at age P28, higher than that of *Nrl*, and both *Nrl* and *Crx* mRNAs were more abundant than beta-actin transcripts (data not shown). Thus, the normal level of *Crx* gene expression in VPA-treated mice appears to be sufficient to drive full expression of *Rho* and *Pde6b* with only 50% *Nrl* expression. This is consistent with the experience of VPA use in humans, which does not decrease visual acuity in patients who do not suffer from retinal degeneration.

Our results also demonstrate that HDAC inhibitors can inhibit, not just promote, retinal gene expression in vivo. Clearly, a simple model where VPA would only act

epigenetically (increase histone acetylation) to increase gene expression is not sufficient to explain the decreases we find in vivo. What are some possible explanations? Photoreceptor development and function requires the coordinated regulation of DNA methylation and histone acetylation as the retina matures [21,29,43]. Chen and Cepko reported that a different HDAC inhibitor, trichostatin-A (TSA), caused severe photoreceptor loss in cultured newborn mouse retinal explants, and TSA also reduced the expression of *Nrl* [22]. They suggested that TSA's effect on *Nrl* gene expression might result from effects on upstream activators of *Nrl* expression or effects on nonhistone protein acetylation. While VPA is a more specific inhibitor of HDACs than TSA, VPA can inhibit at least eight known isoforms: HDAC-1,-2,-3,-4,-5,-7,-8,-9 [16,44]. We suggest that systemic VPA likely reduces *Nrl* gene expression in vivo from effects on nonhistone acetylation as well. HDACs inhibited by VPA have several nonhistone protein substrates that regulate gene expression. Examples are signal transducers and activators of transcription 1 (STAT1), tubulin, and several transcription factors that include CREB, mothers against decapentaplegic homolog 7, transacting transcription factor-1, tumor protein-53, and nuclear factor kappa-B [44]. Thus, a simple de novo prediction of VPA's effect on any individual gene's expression is currently not possible. One must do the experiment.

Systemic VPA can slow the rate of photoreceptor loss in rd1 retinal degeneration mice: Based on previous knowledge, VPA's potential to reduce photoreceptor loss in retinal degeneration is difficult to predict. High systemic doses of VPA were reported to increase the survival of ganglion cells in a rat model of retinal ischemia caused by elevated intraocular pressure [45], but is there any potential for VPA to rescue photoreceptors resulting from an inherent molecular defect? Researchers have proposed that VPA treatment increases neurotrophic factor gene expression in the central nervous system to ameliorate neurologic symptoms in several rodent models of neurodegenerative disease. However, actual measurement of neurotrophic factor gene expression in vivo after VPA treatment is lacking.

Endogenous CNTF and FGF2 (bFGF) protein concentrations increase in response to mechanical damage to the neural retina [46,47]. *Fgf2* gene expression is also elevated in the *Pde6b*^{rd1/rd1} mouse retina [31]. Even though retinal degeneration itself might change neurotrophic factor gene expression, we found that a single systemic dose of VPA could slightly elevate *Gdnf* and *Bdnf* gene expression in the pre-weanling *rd1* mouse retina at an age when some rods were still present. VPA dramatically decreased *Cntf* and *Fgf2* gene expression in the *rd1* neural retina by 80%–90%

compared to PBS-treated littermates. Faced with a mixture of gene expression increases and decreases, we cannot predict VPA's effect on photoreceptor loss in the *rd1* model solely from relative changes in neurotrophic factor gene expression.

Daily systemic VPA treatment of *rd1* mice over an early treatment window (age P9–P21), significantly reduced photoreceptor loss by age P21 (Figure 4A). Daily systemic VPA treatment was as effective as any previously reported treatment using intraocular injection of neurotrophic factors. Because photoreceptor cell fate is determined before age P9 in the mouse, it is unlikely that VPA caused the production of more photoreceptors. To check this possibility, we subjected wild-type mice to the same VPA treatment (from P9 to P21) and found that VPA did not increase photoreceptor numbers during retinal maturation; however, this early VPA treatment did cause a significant thinning of the ONL (Figure 4B). Thus, systemic VPA starting at P9 appears to cause photoreceptor loss in the immature retina *in vivo*, similar to the reported loss of photoreceptors caused by TSA treatment of newborn mouse retinal explants [22]. As previously discussed, VPA treatment of wild-type mice starting later, from P17 to P28, did not result in any photoreceptor loss.

Systemic VPA can accelerate the rate of photoreceptor loss in rd10 retinal degeneration mice: Had we ended our explorations of VPA's effect on photoreceptor loss with the *rd1* mouse strain, one might be encouraged to consider the therapeutic potential of VPA for retinal degeneration in humans. Nevertheless, we hypothesized that VPA might have different effects in retinal degenerations of different etiology. Furthermore, while the *rd1* model is often used to test treatment strategies, both the loss of photoreceptors and the required treatment window overlap completely with the period of retinal and photoreceptor maturation. Our single-dose tests with VPA on pre-weanling wild-type and *rd1* mice reveal that VPA alters the expression of neurotrophic factor and photoreceptor-specific genes. Therefore, it is likely that VPA's benefit in the *rd1* model may result from multiple effects on photoreceptor maturation processes, which are not present in the mature retina. We also examined the *rd10* mouse model. The molecular origin of *rd1* and *rd10* involve the same gene, *Pde6b*, but rod photoreceptors degenerate more slowly in *Pde6b*^{rd10/rd10} mice from age P17 to P40. Compare this to *rd1* where rods degenerate quickly from age P7 to P21. In the case of *Pde6b*^{rd1/rd1} mice, a premature stop codon results in the loss of PDE6B activity. In contrast, *Pde6b*^{rd10/rd10} mice harbor a single point mutation, CGC to TGC in exon-13 of the *Pde6b* gene (Arg560Cys). Typically, several rows of rod photoreceptors still remain at age P28 [28,48]. Unlike *rd1* mice, homozygous *rd10* mice also have a functional visual transduction

pathway, providing the opportunity to test retinal function *in vivo* by ERG.

Both focal ERG and full-field ERG revealed that VPA treatment could not preserve visual function in *Pde6b*^{rd10/rd10} mice. On average, VPA-treated mice had diminished function compared to their PBS-treated littermates. We cannot fully discount the possibility that VPA treatment altered the ERG by affecting phototransduction gene expression. However, systemic VPA treatment of *rd10* mice from age P17 to P28 resulted in a thinner outer nuclear layer in VPA-treated mice compared to their PBS-treated littermates (Figure 8A). Treating *rd10* mice earlier, from P9 to P21, failed to detect any significant difference in ONL thickness between VPA-treated and PBS-treated littermates (Figure 8B). Interestingly, there was a trend (not significant) to increased ONL thickness in the peripheral *rd10* retina when treated earlier. We can only speculate that the relatively less mature peripheral retina was affected differently by VPA, and this may be another indication that VPA impacts photoreceptor maturation processes. The acceleration of photoreceptor loss in the *rd10* model treated later (P17 to P28) is an important result because later treatment did not alter retinal morphology of wild-type mice and the VPA treatment was started when the central retina was mature.

Possible reasons for VPA's differential effect on photoreceptor loss in rd1 and rd10 mice: It is not a new idea that different retinal degeneration models respond differently to chemical treatments, including neurotrophic factor proteins [4]. Using intravitreal injection of proteins, LaVail et al. noted that different neurotrophic factors were effective in different degeneration models and only CNTF slowed photoreceptor loss in the *rd1* model. Frasson et al. and more recently Andrieu-Soler et al. used GDNF protein to slow photoreceptor loss in the *rd1* model [5,10]. Rex et al. also reported a difference with erythropoietin, which enhanced photoreceptor survival in the *Phpr2/rds* (OMIM 179605) model but was not effective in the *rd10* model [49]. However, the failure of VPA to slow photoreceptor loss in the *rd10* model does not mean that this model is untreatable. For example, zinc-desferrioxamine or progestin norgestrel can enhance photoreceptor survival in the *rd10* retina [50,51]. Boatright et al. also reported the attenuation of photoreceptor loss in *rd10* mice using systemic dosing with taurourodeoxycholic acid (TUDCA) [52]. In a different report, TUDCA rescued photoreceptors in *rd10* mice but not *rd1* mice. However, higher doses of TUDCA with side effects were employed in the *rd1* model, leaving this conclusion regarding *rd1* uncertain [53].

In addition to differences in the timing of photoreceptor degeneration relative to the retinal maturation period, the

photoreceptors of *rd1* and *rd10* mice have significantly different physiology. In *rd1* rod photoreceptors, there is an abnormal elevation of cyclic GMP (cGMP) concentration that holds a portion of cyclic nucleotide-gated (CNG) channels in the open state and may elevate intracellular Ca^{2+} concentration. Years before rod phosphodiesterase or its encoding genes were discovered, Farber and Lolly reported the elevation of cGMP in the *rd1* retina before photoreceptor loss and they predicted correctly that this physiologic change was related to the retinal degeneration [54]. The normal activities of rhodopsin, transducin, and arrestin are altered from changes to intracellular Ca^{2+} concentration. In contrast to *rd1*, the *rd10* rod photoreceptor has some phosphodiesterase activity, light-mediated regulation of cGMP and Ca^{2+} concentrations, and visual transduction.

In the case of VPA, it is also possible that the inhibition of *Nrl* gene expression during the photoreceptor maturation phase leads to a slight delay in the expression of *Rhodopsin* and other photoreceptor genes. This effect might be more crucial in the *rd1* retina when dosing is started at age P9 and less consequential in the *rd10* retina when dosing began at age P17. Thus, it is possible that *rd1* photoreceptors mature more slowly under systemic VPA treatment and thus avoid some physiologic stress resulting in a slower rate of photoreceptor loss. CNTF protein exposure is known to inhibit the birth of rods in the developing retina via the activation of STAT3 signaling [55,56], but this effect is upon photoreceptor progenitor cells. More than 95% of rods are born (postmitotic) by the time we have started our earliest VPA treatment in vivo at P9. Wahlin et al. found that injections of CNTF, BDNF, or FGF2 activated detectable signal transduction (pCREB, pERK, and cFOS) only in cells of the mature rodent INL [57]. The degree to which changes of neurotrophic factor gene expression may affect photoreceptor maturation in the *rd1* model is not clear, but developmental effects are another possible mechanism of VPA's photoreceptor rescue.

Regardless of the specific reasons for the different effect of systemic VPA treatment on photoreceptor survival in these two mouse models, our results demonstrate that the context of photoreceptor development and physiology can result in different effects on the rate of photoreceptor loss. Considering that VPA treatment of the *rd10* model from P17 to P28 avoided the early toxicity seen when starting treatment of wild-type mice at P9 and that the central retina is essentially mature by age P17, then the disadvantage of systemic VPA treatment with the *rd10* model would indicate some need for caution when testing human RP patients.

Two recent retrospective studies of RP patients receiving VPA have reported different results. Clemson et al. reported

an increase in visual acuity [23]. In contrast, Bhalla et al. reported a possible visual field loss and an average reduction in visual acuity in patients taking VPA for 14 months [58]. Without placebo groups, these mixed results from small numbers of patients are inconclusive about VPA's possible efficacy or disadvantage for the RP patient. We do know that there is extensive genetic heterogeneity involved in retinal degenerations [1], and so it is possible that VPA could benefit or harm depending on the underlying disease etiology. For example, the first reported NRL mutation *NRL^{s50t}* results in abnormally higher transactivation activity of rod-specific gene promoters in vitro [40]. If such patients were included in the current clinical trials, would reducing *NRL^{s50t}* gene expression with VPA reduce NRL activity and the rate of rod photoreceptor loss? We cannot make such predictions with our current state of knowledge. Without a specific animal model for this or other RP mutations, the safest approach will be clinical trials that compare treatment and placebo between individuals sharing the same disease etiology while monitoring for any disadvantage from VPA treatment.

APPENDIX 1. SYSTEMIC VPA TREATMENT OF WILD-TYPE MICE FROM P17-P28 (LATER TREATMENT) HAD NO EFFECT ON RETINAL MORPHOLOGY.

To access the data, click or select the words "[Appendix 1.](#)" Examples of b-scans are shown from VPA-treated and PBS-treated littermates. Average ONL (outer nuclear layer) thickness was the same between both groups. Using InVivoVue Diver software, 24 different measurement locations were obtained from a 5×5 rectangular grid (1.4×1.4 mm, measurement was not made at one grid position centered on the optic disc.) The average ONL thicknesses were: 63±2 μm for PBS-treated littermates (n=3 mice) and 63±2 μm for VPA-treated littermates (n=3 mice). Vertical (red) and horizontal (green) scale bars represent millimeters.

APPENDIX 2. EXAMPLE VIRTUAL MICROSCOPY RETINAL SECTION FROM A PBS-TREATED *PDE6B^{RD1/RD1}* (CONTROL) LITTERMATE.

To access the data, click or select the words "[Appendix 2.](#)" Age P21. Scanned using a 20× objective lens with an Olympus SL120 Virtual Microscopy Slide Scanner. The full section representation is digitally assembled from about nine separate image fields per retina section.

APPENDIX 3. EXAMPLE OF VIRTUAL MICROSCOPY RETINAL SECTION FROM A VPA-TREATED *PDE6B*^{RD1/R1} LITTERMATE.

To access the data, click or select the words “Appendix 3.” Age P21. Scanned using a 20× objective lens with an Olympus SL120 Virtual Microscopy Slide Scanner. The full section representation is digitally assembled from about nine separate images per retina section.

APPENDIX 4. VIRTUAL MICROSCOPY IMAGES FROM A REPEATED TRIAL OF LATER VPA-TREATMENT (P17-P28) WITH THE *PDE6B*^{RD10/RD10} MOUSE STRAIN.

To access the data, click or select the words “Appendix 4.” Central retinas from two different PBS-treated and two different VPA-treated littermates are shown. This repeated experiment confirmed that VPA-treatment resulted in a thinner ONL relative to PBS-treated littermates.

ACKNOWLEDGMENTS

The authors thank: Greg Sprehn (Phoenix Research Labs, currently at Rivendell Heights, Inc.) and Bert Massie (Phoenix Research Labs) for help with focal ERG software adaptation and focal-ERG light calibration; Paula Pierce of Excalibur laboratories for tissue sectioning and staining of slides in suitable format for our Olympus slide scanner; undergraduate student Keriah Abd for assistance during mouse ERGs; and David Zhu (Oakland University/William Beaumont School of Medicine) for maintaining operations of the virtual microscopy server. Funding supporting aspects of this research were provided by: the Center for Biomedical Research, Oakland University, Research Excellence Award (K.P.M.); Vision Research ROPARD Foundation Facility Support Award (Eye Research Institute, Oakland University); and the National Institutes of Health, NEI grant R01EY014626 (K.P.M.).

REFERENCES

- Berger W, Kloeckener-Gruissem B, Neidhardt J. The molecular basis of human retinal and vitreoretinal diseases. *Prog Retin Eye Res* 2010; 29:335-75. [PMID: 20362068].
- Cideciyan AV, Jacobson SG, Beltran WA, Sumaroka A, Swider M, Iwabe S, Roman AJ, Olivares MB, Schwartz SB, Komaromy AM, Hauswirth WW, Aguirre GD. Human retinal gene therapy for leber congenital amaurosis shows advancing retinal degeneration despite enduring visual improvement. *Proc Natl Acad Sci USA* 2013; 110:E517-25. [PMID: 23341635].
- Azadi S, Johnson LE, Paquet-Durand F, Perez MT, Zhang Y, Ekstrom PA, van Veen T. Cntf+Bdnf treatment and neuroprotective pathways in the rd1 mouse retina. *Brain Res* 2007; 1129:116-29. [PMID: 17156753].
- LaVail MM, Yasumura D, Matthes MT, Lau-Villacorta C, Unoki K, Sung CH, Steinberg RH. Protection of mouse photoreceptors by survival factors in retinal degenerations. *Invest Ophthalmol Vis Sci* 1998; 39:592-602. [PMID: 9501871].
- Frasson M, Picaud S, Leveillard T, Simonutti M, Mohand-Said S, Dreyfus H, Hicks D, Sabel J. Glial cell line-derived neurotrophic factor induces histologic and functional protection of rod photoreceptors in the rd/rd mouse. *Invest Ophthalmol Vis Sci* 1999; 40:2724-34. [PMID: 10509671].
- Ezzeddine ZD, Yang X, DeChiara T, Yancopoulos G, Cepko CL. Postmitotic cells fated to become rod photoreceptors can be respecified by cntf treatment of the retina. *Development* 1997; 124:1055-67. [PMID: 9056780].
- Kirsch M, Schulz-Key S, Wiese A, Fuhrmann S, Hofmann H. Ciliary neurotrophic factor blocks rod photoreceptor differentiation from postmitotic precursor cells in vitro. *Cell Tissue Res* 1998; 291:207-16. [PMID: 9426308].
- Kirsch M, Fuhrmann S, Wiese A, Hofmann HD. Cntf exerts opposite effects on in vitro development of rat and chick photoreceptors. *Neuroreport* 1996; 7:697-700. [PMID: 8733724].
- Tao W, Wen R, Goddard MB, Sherman SD, O'Rourke PJ, Stabila PF, Bell WJ, Dean BJ, Kauper KA, Budz VA, Tsiaras WG, Acland GM, Pearce-Kelling S, Laties AM, Aguirre GD. Encapsulated cell-based delivery of Cntf reduces photoreceptor degeneration in animal models of retinitis pigmentosa. *Invest Ophthalmol Vis Sci* 2002; 43:3292-8. [PMID: 12356837].
- Andrieu-Soler C, Aubert-Pouessel A, Doat M, Picaud S, Halhal M, Simonutti M, Venier-Julienne MC, Benoit JP, Behar-Cohen F. Intravitreal injection of plga microspheres encapsulating gdnf promotes the survival of photoreceptors in the rd1/rd1 mouse. *Mol Vis* 2005; 11:1002-11. [PMID: 16319820].
- Braiteh F, Soriano AO, Garcia-Manero G, Hong D, Johnson MM, Silva Lde P, Yang H, Alexander S, Wolff J, Kurzrock R. Phase 1 study of epigenetic modulation with 5-azacytidine and valproic acid in patients with advanced cancers. *Clin Cancer Res* 2008; 14:6296-301. [PMID: 18829512].
- Issa JP, Kantarjian HM. Targeting DNA methylation. *Clin Cancer Res* 2009; 15:3938-46. [PMID: 19509174].
- Phiel CJ, Zhang F, Huang EY, Guenther MG, Lazar MA, Klein PS. Histone deacetylase is a direct target of valproic acid, a potent anticonvulsant, mood stabilizer, and teratogen. *J Biol Chem* 2001; 276:36734-41. [PMID: 11473107].
- Mitton KP, Guzman AE. Focus on molecules: 5-methylcytosine, a possible epigenetic link between ageing and ocular disease. *Exp Eye Res* 2012; 96:2-3. [PMID: 20620139].
- Feng HL, Leng Y, Ma CH, Zhang J, Ren M, Chuang DM. Combined lithium and valproate treatment delays disease onset, reduces neurological deficits and prolongs survival in

- an amyotrophic lateral sclerosis mouse model. *Neuroscience* 2008; 155:567-72. [PMID: 18640245].
16. Chuang DM, Leng Y, Marinova Z, Kim HJ, Chiu CT. Multiple roles of hdac inhibition in neurodegenerative conditions. *Trends Neurosci* 2009; 32:591-601. [PMID: 19775759].
 17. Wu X, Chen PS, Dallas S, Wilson B, Block ML, Wang CC, Kinyamu H, Lu N, Gao X, Leng Y, Chuang DM, Zhang W, Lu RB, Hong JS. Histone deacetylase inhibitors up-regulate astrocyte Gdnf and Bdnf gene transcription and protect dopaminergic neurons. *Int J Neuropsychopharmacol* 2008; 11:1123-34. [PMID: 18611290].
 18. Zhang ZZ, Gong YY, Shi YH, Zhang W, Qin XH, Wu XW. Valproate promotes survival of retinal ganglion cells in a rat model of optic nerve crush. *Neuroscience* 2012; [PMID: 22867974].
 19. Liou GI, Wang M, Matragoon S. Timing of interphotoreceptor retinoid-binding protein (Irbp) gene expression and hypomethylation in developing mouse retina. *Dev Biol* 1994; 161:345-56. [PMID: 8313988].
 20. Peng GH, Chen S. Crx activates opsin transcription by recruiting hat-containing co-activators and promoting histone acetylation. *Hum Mol Genet* 2007; 16:2433-52. [PMID: 17656371].
 21. Cvekl A, Mitton KP. Epigenetic regulatory mechanisms in vertebrate eye development and disease. *Heredity* 2010; 105:135-51. [PMID: 20179734].
 22. Chen B, Cepko CL. Requirement of histone deacetylase activity for the expression of critical photoreceptor genes. *BMC Dev Biol* 2007; 7:78-[PMID: 17603891].
 23. Clemson CM, Tzekov R, Krebs M, Checchi JM, Bigelow C, Kaushal S. Therapeutic potential of valproic acid for retinitis pigmentosa. *Br J Ophthalmol* 2011; [PMID: 20647559].
 24. Geller AM, Hudnell HK, Vaughn BV, Messenheimer JA, Boyes WK. Epilepsy and medication effects on the pattern visual evoked potential. *Doc Ophthalmol* 2005; 110:121-31. [PMID: 16249963].
 25. Verrotti A, Lobefalo L, Priolo T, Rapinese M, Trotta D, Morgese G, Gallenga PE, Chiarelli F. Color vision in epileptic adolescents treated with valproate and carbamazepine. *Seizure* 2004; 13:411-7. [PMID: 15276145].
 26. Bayer AU, Thiel HJ, Zrenner E, Dichgans J, Kuehn M, Paulus W, Ried S, Schmidt D. Color vision tests for early detection of antiepileptic drug toxicity. *Neurology* 1997; 48:1394-7. [PMID: 9153479].
 27. Goto Y, Taniwaki T, Shigematsu J, Tobimatsu S. The long-term effects of antiepileptic drugs on the visual system in rats: Electrophysiological and histopathological studies. *Clin Neurophysiol* 2003; 114:1395-402. [PMID: 12888021].
 28. Chang B, Hawes NL, Pardue MT, German AM, Hurd RE, Davisson MT, Nusinowitz S, Rengarajan K, Boyd AP, Sidney SS, Phillips MJ, Stewart RE, Chaudhury R, Nickerson JM, Heckenlively JR, Boatright JH. Two mouse retinal degenerations caused by missense mutations in the beta-subunit of rod cGMP phosphodiesterase gene. *Vision Res* 2007; 47:624-33. [PMID: 17267005].
 29. Hao H, Tummala P, Guzman E, Mali RS, Gregorski J, Swaroop A, Mitton KP. The transcription factor neural retina leucine zipper (Nrl) controls photoreceptor-specific expression of myocyte enhancer factor Mef2c from an alternative promoter. *J Biol Chem* 2011; 286:34893-902. [PMID: 21849497].
 30. Gao H, Hollyfield JG. Basic fibroblast growth factor in retinal development: Differential levels of bFGF expression and content in normal and retinal degeneration (rd) mutant mice. *Dev Biol* 1995; 169:168-84. [PMID: 7750636].
 31. Gao H, Hollyfield JG. Basic fibroblast growth factor: Increased gene expression in inherited and light-induced photoreceptor degeneration. *Exp Eye Res* 1996; 62:181-9. [PMID: 8698078].
 32. Bowes C, Li T, Danciger M, Baxter LC, Applebury ML, Farber DB. Retinal degeneration in the rd mouse is caused by a defect in the beta subunit of rod cGMP-phosphodiesterase. *Nature* 1990; 347:677-80. [PMID: 1977087].
 33. Bowes C, Danciger M, Kozak CA, Farber DB. Isolation of a candidate Cdna for the gene causing retinal degeneration in the rd mouse. *Proc Natl Acad Sci USA* 1989; 86:9722-6. [PMID: 2481314].
 34. Tummala P, Mali RS, Guzman E, Zhang X, Mitton KP. Temporal chip-on-chip of RNA-Polymerase-II to detect novel gene activation events during photoreceptor maturation. *Mol Vis* 2010; 16:252-71. [PMID: 20161818].
 35. Yasuda S, Liang MH, Marinova Z, Yahyavi A, Chuang DM. The mood stabilizers lithium and valproate selectively activate the promoter IV of brain-derived neurotrophic factor in neurons. *Mol Psychiatry* 2009; 14:51-9. [PMID: 17925795].
 36. Chen PS, Peng GS, Li G, Yang S, Wu X, Wang CC, Wilson B, Lu RB, Gean PW, Chuang DM, Hong JS. Valproate protects dopaminergic neurons in midbrain neuron/glia cultures by stimulating the release of neurotrophic factors from astrocytes. *Mol Psychiatry* 2006; 11:1116-25. [PMID: 16969367].
 37. Oh EC, Cheng H, Hao H, Jia L, Khan NW, Swaroop A. Rod differentiation factor nrl activates the expression of nuclear receptor Nr2e3 to suppress the development of cone photoreceptors. *Brain Res* 2008; 1236:16-[PMID: 18294621].
 38. Oh EC, Khan N, Novelli E, Khanna H, Strettoi E, Swaroop A. Transformation of cone precursors to functional rod photoreceptors by bzip transcription factor Nrl. *Proc Natl Acad Sci USA* 2007; 104:1679-84. [PMID: 17242361].
 39. Mears AJ, Kondo M, Swain PK, Takada Y, Bush RA, Saunders TL, Sieving PA, Swaroop A. Nrl is required for rod photoreceptor development. *Nat Genet* 2001; 29:447-52. [PMID: 11694879].
 40. Bessant DA, Payne AM, Mitton KP, Wang QL, Swain PK, Plant C, Bird AC, Zack DJ, Swaroop A, Bhattacharya SS. A mutation in Nrl is associated with autosomal dominant retinitis pigmentosa. *Nat Genet* 1999; 21:355-6. [PMID: 10192380].

41. Mitton KP, Swain PK, Chen S, Xu S, Zack DJ, Swaroop A. The leucine zipper of nrl interacts with the Crx homeodomain. A possible mechanism of transcriptional synergy in rhodopsin regulation. *J Biol Chem* 2000; 275:29794-9. [PMID: 10887186].
42. Mali RS, Zhang X, Hoerauf W, Doyle D, Devitt J, Loffreda-Wren J, Mitton KP. Fiz1 is expressed during photoreceptor maturation, and synergizes with Nrl and Crx at rod-specific promoters in vitro. *Exp Eye Res* 2007; 84:349-60. [PMID: 17141759].
43. Rai K, Jafri IF, Chidester S, James SR, Karpf AR, Cairns BR, Jones DA. Dnmt3 and G9a cooperate for tissue-specific development in zebrafish. *J Biol Chem* 2010; 285:4110-21. [PMID: 19946145].
44. Itoh Y, Suzuki T, Miyata N. Isoform-selective histone deacetylase inhibitors. *Curr Pharm Des* 2008; 14:529-44. [PMID: 18336298].
45. Zhang Z, Qin X, Tong N, Zhao X, Gong Y, Shi Y, Wu X. Valproic acid-mediated neuroprotection in retinal ischemia injury via histone deacetylase inhibition and transcriptional activation. *Exp Eye Res* 2012; 94:98-108. [PMID: 22143029].
46. Wen R, Song Y, Cheng T, Matthes MT, Yasumura D, LaVail MM, Steinberg RH. Injury-induced upregulation of bFGF and Cntf mRNAs in the rat retina. *J Neurosci* 1995; 15:7377-85. [PMID: 7472491].
47. Walsh N, Valter K, Stone J. Cellular and subcellular patterns of expression of bFGF and Cntf in the normal and light stressed adult rat retina. *Exp Eye Res* 2001; 72:495-501. [PMID: 11311041].
48. Chang B, Hawes NL, Hurd RE, Davisson MT, Nusinowitz S, Heckenlively JR. Retinal degeneration mutants in the mouse. *Vision Res* 2002; 42:517-25. [PMID: 11853768].
49. Rex TS, Allocca M, Domenici L, Surace EM, Maguire AM, Lyubarsky A, Cellierino A, Bennett J, Auricchio A. Systemic but not intraocular epo gene transfer protects the retina from light-and genetic-induced degeneration. *Molecular Gene Therapy*. 2004; 10:855-61. .
50. Obolensky A, Berenshtein E, Lederman M, Bulvik B, Alper-Pinus R, Yaul R, Deleon E, Chowers I, Chevion M, Banin E. Zinc-desferrioxamine attenuates retinal degeneration in the rd10 mouse model of retinitis pigmentosa. *Free Radic Biol Med* 2011; 51:1482-91. [PMID: 21824515].
51. Doonan F, O'Driscoll C, Kenna P, Cotter TG. Enhancing survival of photoreceptor cells in vivo using the synthetic progestin norgestrel. *J Neurochem* 2011; 118:915-27. [PMID: 21689103].
52. Boatright JH, Moring AG, McElroy C, Phillips MJ, Do VT, Chang B, Hawes NL, Boyd AP, Sidney SS, Stewart RE, Minear SC, Chaudhury R, Ciavatta VT, Rodrigues CM, Steer CJ, Nickerson JM, Pardue MT. Tool from ancient pharmacopoeia prevents vision loss. *Mol Vis* 2006; 12:1706-14. [PMID: 17213800].
53. Drack AV, Dumitrescu AV, Bhattarai S, Gratie D, Stone EM, Mullins R, Sheffield VC. TUDCA slows retinal degeneration in two different mouse models of retinitis pigmentosa and prevents obesity in Bardet-Biedl syndrome type 1 mice. *Invest Ophthalmol Vis Sci* 2012; 53:100-6. [PMID: 22110077].
54. Farber DB, Lolley RN. Cyclic guanosine monophosphate: Elevation in degenerating photoreceptor cells of the C3h mouse retina. *Science* 1974; 186:449-51. [PMID: 4369896].
55. Ozawa Y, Nakao K, Shimazaki T, Takeda J, Akira S, Ishihara K, Hirano T, Oguchi Y, Okano H. Downregulation of Stat3 activation is required for presumptive rod photoreceptor cells to differentiate in the postnatal retina. *Mol Cell Neurosci* 2004; 26:258-70. [PMID: 15207851].
56. Zhang SS, Liu MG, Kano A, Zhang C, Fu XY, Barnstable CJ. Stat3 activation in response to growth factors or cytokines participates in retina precursor proliferation. *Exp Eye Res* 2005; 81:103-15. [PMID: 15978261].
57. Wahlin KJ, Adler R, Zack DJ, Campochiaro PA. Neurotrophic signaling in normal and degenerating rodent retinas. *Exp Eye Res* 2001; 73:693-701. [PMID: 11747369].
58. Bhalla S, Joshi D, Bhullar S, Kasuga D, Park Y, Kay CN. Long-term follow-up for efficacy and safety of treatment of retinitis pigmentosa with valproic acid. *Br J Ophthalmol* 2013; 97:895-9. [PMID: 23603755].

Articles are provided courtesy of Emory University and the Zhongshan Ophthalmic Center, Sun Yat-sen University, P.R. China. The print version of this article was created on 4 November 2014. This reflects all typographical corrections and errata to the article through that date. Details of any changes may be found in the online version of the article.